THE BOUNDARY FINITE ELEMENT METHOD FOR THE SEMI-ANALYTICAL COMPUTATION OF 3D STRESS SINGULARITIES IN FRACTURE MECHANICS

C. Mittelstedt[1] & W. Becker[2]
[1]Siegen University, Department of Mechanical Engineering, Paul-Bonatz-Str. 9-11, D-57068 Siegen, Germany.
[2]Darmstadt University of Technology, Department of Mechanics, Hochschulstr. 1, D-64289 Darmstadt, Germany.

ABSTRACT

The numerical analysis of singular elasticity problems by means of standard finite element analyses usually requires significant computational effort, hence there is a particular interest in introducing new and efficient analysis methods like e.g. the boundary finite element method (BFEM, [1]), especially when detailed information on the asymptotic behaviour of the state variables – displacements, strains and stresses – in the vicinity of the singularity is sought. The BFEM combines the advantages of the finite element method and the boundary element method to a new and efficient procedure.

As a prerequisite the BFEM assumes a certain scalability of the given structure with respect to a similarity center. In analogy to the boundary element method, only the boundary of the structure needs to be discretized, wherein standard isoparametric displacement based finite element formulations are sufficient. Thus, no fundamental solution is required. Hence, the BFEM can be characterized as a fundamental-solution-less boundary element method solely based on finite elements. In the course of the finite element based derivation of the governing equations, the similarity or scalability characteristics enable a separation of coordinates such that in the scaling direction the method yields simple systems of differential equations that can be solved in an analytical way. In the directions perpendicular to the scaling direction the method converges in the FEM sense. The BFEM thus exhibits semi-analytical characteristics.

In the present contribution the BFEM is employed for the investigation of the order of stress singularities for several classes of three-dimensional singular stress concentration problems, e.g. for three-dimensional crack [2-4] or notch [5] situations as well as for free edges [6] and corners [7,8] of layered structures. In all cases, the BFEM results agree excellently with reference results. The required computational effort is considerably lower compared to e.g. standard FEM computations and thus establishes the BFEM as a powerful tool for the numerical modelling of linear elastic solids.

1 THE BOUNDARY FINITE ELEMENT METHOD (BFEM)

The BFEM is a boundary element method based on standard finite element formulations and does not require a fundamental solution. It applies for the investigation of unbounded as well as bounded structures and uses scalability of the given structure with respect to a similarity center S. In order to introduce the basics of the BFEM let us consider a free corner interface between two arbitrary layers of a laminated plate (fig. 1) the geometry of which can be described by the introduction of a fictitious convex interior boundary Γ_i of arbitrary shape at the characteristic radial distance r_i from the similarity center S, and a centric scaling of the radial coordinate r so that the radial coordinate r_e of an arbitrary similar exterior boundary Γ_e is described by $r_e = (1+w)r_i$. The quantity w is a dimensionless scaling parameter. The resultant space between Γ_i and Γ_e (so-called finite element cell) is discretized with one single layer of standard displacement based isoparametric finite volume elements. Note that presently the similarity center is identical to the singular point in the interface of the three-dimensional laminate corner situation where considerable stress singularities are known to occur [6-8]. The force-displacement relation

concerning the finite element cell reads in a decomposed notation with respect to the interior and exterior boundary:

$$\begin{bmatrix} \mathbf{K}_{ii} & \mathbf{K}_{ie} \\ \mathbf{K}_{ei} & \mathbf{K}_{ee} \end{bmatrix} \begin{pmatrix} \mathbf{u}_i \\ \mathbf{u}_e \end{pmatrix} = \begin{pmatrix} \mathbf{F}_i \\ \mathbf{F}_e \end{pmatrix}. \tag{1}$$

The stiffness submatrices $\mathbf{K}_{jl}$ with $j,l = i,e$ read:

$$\mathbf{K}_{jl} = \int_{-1}^{+1} \int_{-1}^{+1} \int_{-1}^{+1} \mathbf{B}_j^T \mathbf{C} \mathbf{B}_l \det(\mathbf{J}) \mathrm{d}\xi \mathrm{d}\eta \mathrm{d}\zeta, \tag{2}$$

wherein $\mathbf{C}$ is the stiffness matrix of the layer material and $\det(\mathbf{J})$ denotes the determinant of the Jacobian matrix. The natural element coordinates are introduced as ξ, η, ζ, wherein ξ is the local radial coordinate parallel to r, the circumferential directions are denoted as η, ζ. The strain-displacement operator matrices $\mathbf{B}_j$ and $\mathbf{B}_l$ are derived straightforwardly by employing a consequent decomposition of the element formulations into portions concerning the interior and exterior boundary. Details can be found in e.g. [1]. The arrays $\mathbf{u}_i$, $\mathbf{u}_e$ and $\mathbf{F}_i$, $\mathbf{F}_e$ contain the nodal displacements and forces on the boundaries Γ_i and Γ_e.

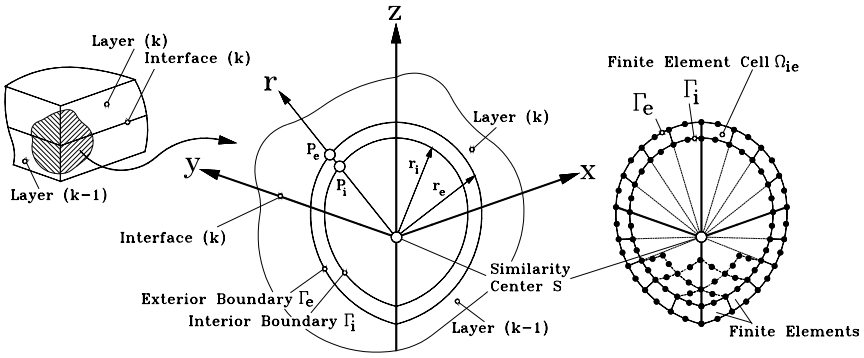

Figure 1: Principle of scalability and discretization of a 3D interface corner.

With respect to the radial coordinate ξ the integration process eqn (2) can be easily performed in an analytical manner as the integrand is a polynomial in ξ. When a linear displacement representation is chosen in the scaling direction, the following result for $\mathbf{K}_{jl}$ is achieved (with $\xi_i = -1$ and $\xi_e = +1$):

$$\mathbf{K}_{jl} = \tfrac{\xi_j \xi_l}{w} \mathbf{E}^0 + \xi_j \xi_l \mathbf{E}^0 + \tfrac{\xi_l}{2} \mathbf{E}^1 + \tfrac{\xi_j}{2} \mathbf{E}^{1^T} + w\left(\tfrac{\xi_j \xi_l}{3} \mathbf{E}^0 + \left(\tfrac{\xi_l}{4} + \tfrac{\xi_j \xi_l}{12} \right) \mathbf{E}^1 + \left(\tfrac{\xi_j}{4} + \tfrac{\xi_j \xi_l}{12} \right) \mathbf{E}^{1^T} + \left(\tfrac{1}{4} + \tfrac{\xi_j \xi_l}{12} \right) \mathbf{E}^2 \right). \tag{3}$$

The matrices $\mathbf{E}^0$, $\mathbf{E}^1$, $\mathbf{E}^2$ solely depend on η, ζ and on the finite element meshes on the boundaries:

$$\mathbf{E}^0 = \int_{-1}^{+1} \int_{-1}^{+1} \mathbf{B}^{1^T} \mathbf{C} \mathbf{B}^1 \det(\mathbf{J}) \mathrm{d}\eta \mathrm{d}\zeta, \quad \mathbf{E}^1 = \int_{-1}^{+1} \int_{-1}^{+1} \mathbf{B}^{2^T} \mathbf{C} \mathbf{B}^1 \det(\mathbf{J}) \mathrm{d}\eta \mathrm{d}\zeta,$$

$$\mathbf{E}^2 = \int_{-1}^{+1} \int_{-1}^{+1} \mathbf{B}^{2^T} \mathbf{C} \mathbf{B}^2 \det(\mathbf{J}) \mathrm{d}\eta \mathrm{d}\zeta. \tag{4}$$

The operator matrices $\mathbf{B}^1$ and $\mathbf{B}^2$ incorporate partial derivatives of the finite element shape functions, see [1] for more details. Equilibrium between the finite element cell and the enclosing actual structure leads to the following force-displacement relationship:

$$\begin{bmatrix} \mathbf{K}_{ii} & \mathbf{K}_{ie} \\ \mathbf{K}_{ei} & \mathbf{K}_{ee} \end{bmatrix} \begin{pmatrix} \mathbf{u}_i \\ \mathbf{u}_e \end{pmatrix} = \begin{pmatrix} \mathbf{F}_i \\ \mathbf{F}_e \end{pmatrix} = \begin{bmatrix} \mathbf{K}_i & 0 \\ 0 & -\mathbf{K}_e \end{bmatrix} \begin{pmatrix} \mathbf{u}_i \\ \mathbf{u}_e \end{pmatrix}. \tag{5}$$

The two unknown boundary stiffness matrices $\mathbf{K}_i$ and $\mathbf{K}_e$ describe the deformation behaviour of the unbounded structures characterized by the boundaries Γ_i and Γ_e. After the elimination of e.g. $\mathbf{u}_e$

from eqn (5) and the choice of an arbitrary $\mathbf{u}_i$, the scaling property $\mathbf{K}_e = (1+w)\mathbf{K}_i$ relating the two unknown boundary stiffness matrices and the limit $w \to 0$ lead to an algebraic matrix Riccati equation for the boundary stiffness matrix $\mathbf{K} = \mathbf{K}_i$:

$$\mathbf{K}\mathbf{E}^{0^{-1}}\mathbf{K} + \left(\mathbf{E}^1\mathbf{E}^{0^{-1}} - \tfrac{1}{2}\mathbf{I}\right)\mathbf{K} + \mathbf{K}\left(\mathbf{E}^{0^{-1}}\mathbf{E}^{1^T} - \tfrac{1}{2}\mathbf{I}\right) - \mathbf{E}^2 + \mathbf{E}^1\mathbf{E}^{0^{-1}}\mathbf{E}^{1^T} = 0, \tag{6}$$

wherein we have introduced the identity matrix $\mathbf{I}$. We determine a solution from the equivalent eigenvalue problem which reads:

$$\begin{pmatrix} -\mathbf{E}^{0^{-1}}\mathbf{E}^{1^T} + \tfrac{1}{2}\mathbf{I} & -\mathbf{E}^{0^{-1}} \\ -\mathbf{E}^2 + \mathbf{E}^1\mathbf{E}^{0^{-1}}\mathbf{E}^{1^T} & \mathbf{E}^1\mathbf{E}^{0^{-1}} - \tfrac{1}{2}\mathbf{I} \end{pmatrix} \begin{pmatrix} \mathbf{\Phi}_{11} & \mathbf{\Phi}_{12} \\ \mathbf{\Phi}_{21} & \mathbf{\Phi}_{22} \end{pmatrix} = \begin{pmatrix} \mathbf{\Phi}_{11} & \mathbf{\Phi}_{12} \\ \mathbf{\Phi}_{21} & \mathbf{\Phi}_{22} \end{pmatrix} \begin{pmatrix} \boldsymbol{\lambda} & \mathbf{0} \\ \mathbf{0} & -\boldsymbol{\lambda} \end{pmatrix}. \tag{7}$$

Herein, $\mathbf{\Phi}_{11}$, $\mathbf{\Phi}_{12}$, $\mathbf{\Phi}_{21}$, $\mathbf{\Phi}_{22}$ are submatrices of the matrix of eigenvectors, the diagonal matrix $\boldsymbol{\lambda}$ includes the corresponding eigenvalues. The boundary stiffness matrix $\mathbf{K} = \mathbf{K}_i$ then results in:

$$\mathbf{K} = \mathbf{\Phi}_{21}\mathbf{\Phi}_{11}^{-1}. \tag{8}$$

The first of eqns (5) finally yields a system of non-linear first order differential equations for the displacements after again performing the limit $w \to 0$:

$$r\mathbf{u}_{,r} = \left(\mathbf{\Phi}_{11}\boldsymbol{\lambda}\mathbf{\Phi}_{11}^{-1} - \tfrac{1}{2}\mathbf{I}\right)\mathbf{u}. \tag{9}$$

A closed-form solution is possible and with the boundary displacements $\mathbf{u}_0$ reads:

$$\mathbf{u} = \mathbf{\Phi}_{11}\mathrm{diag}\left(\left(\tfrac{r}{r_0}\right)^{\lambda_i - \frac{1}{2}}\right)\mathbf{\Phi}_{11}^{-1}\mathbf{u}_0. \tag{10}$$

From the displacement solution eqn (10), strains and stresses are obtainable. After performing the limit $w \to 0$ and solving the matrix Riccati equation, the BFEM basically consists of the introduction of a pattern of surface elements on the boundary of the structure only, hence reducing the spatial dimension of discretization by one. An analytical solution for the displacements with respect to the radial coordinate is possible, in the circumferential directions the BFEM converges in the FEM sense, thus rendering the BFEM a semi-analytical method.

2 RESULTS FOR THREE-DIMENSIONAL STRESS SINGULARITIES

The BFEM incorporates singular stresses in a natural way due to the power law form of the displacement solution eqn (10). Hence, the BFEM can be used efficiently in particular for the asymptotic investigation of stress singularities for several classes of elasticity problems for which the displacements and stresses are usually formulated as infinite series in variable separable form:

$$u_i = \sum_{m=1}^{m=\infty} K_m r^{\lambda_m} g_{im}(\varphi_1, \varphi_2), \quad \sigma_{ij} = \sum_{m=1}^{m=\infty} K_m r^{\lambda_m - 1} f_{ijm}(\varphi_1, \varphi_2). \tag{11}$$

Herein, we have introduced a spherical coordinate system r, φ_1, φ_2, with r being the radial direction. At the point $r = 0$ a stress singularity is assumed to occur. For the behaviour of the state variables a power law form is assumed, the angular variations are described by the functions g_{im} and f_{ijm}. The quantities K_m are generalized stress intensity factors, the λ_m are eigenvalues that may be either real or complex. When $\mathrm{Re}(\lambda_m) < 1$ the stresses become singular when $r \to 0$. Due to energetic reasons only eigenvalues fulfilling $0 < \mathrm{Re}\,(\lambda_m) < 1$ are of interest. The order of stress singularity is then calculated as the exponent λ_m - 1 of the stress representation.

2.1 Stress singularities at the vertex of a surface breaking crack

The situation of a surface crack in an isotropic halfspace with the crack front perpendicular to the free surface (fig. 2, upper left portion) is a well-known benchmark example within the context of three-dimensional fracture mechanics. Numerical results for the order of the occurring stress

singularity at the crack vertex have been reported by e.g. Somaratna / Ting [2] or Dimitrov et al. [4]. The similarity center is presently placed at the crack vertex at $x = y = z = 0$. The cracked halfspace is situated in the region $r \geq 0$, $0 \leq \varphi_1 \leq \pi/2$, $0 \leq \varphi_2 \leq 2\pi$. The areas $r \geq 0$, $0 \leq \varphi_1 \leq \pi/2$, $\varphi_2 = 0$ and $r \geq 0$, $0 \leq \varphi_1 \leq \pi/2$, $\varphi_2 = 2\pi$ are the stress free crack surfaces, the crack front runs parallel to the positive z-axis. The stress free surface of the halfspace is situated at $z = 0$. The surface Γ of a unit sphere at $r = 1$ has been discretized with 8-noded quadrangular surface elements wherein a mesh refinement has been applied in the vicinity of the point $x = y = 0$, $z = 1$ where the crack front intersects with the discretized surface Γ. The symmetry of the given situation has been considered for a reduction of the computational effort: for symmetric deformation modes the displacements u_2 were prescribed as $u_2 = 0$ on the symmetry line Γ_s, for unsymmetric deformation modes $u_r = u_1 = 0$ holds on Γ_s. Thus, only one half of the crack situation had to be discretized, e.g. enclosed in the range $r = 1$, $0 \leq \varphi_1 \leq \pi/2$, $0 \leq \varphi_2 \leq \pi$. We have varied Poisson's ratio of the assumed isotropic material and found three eigenvalues λ with $0 < \mathrm{Re}(\lambda) < 1$ in the range $0 < \nu < 0.3$ (fig. 2, upper right portion). For values above approximately $\nu = 0.3$, only two relevant eigenvalues remain. Note that the dominating eigenvalue exceeds the well-known $r^{-0.5}$-singularity of the two-dimensional Griffith-crack situation in all cases. In all, the BFEM computations show a good conformity with the results of Somaratna / Ting [2] and Dimitrov et al. [4].

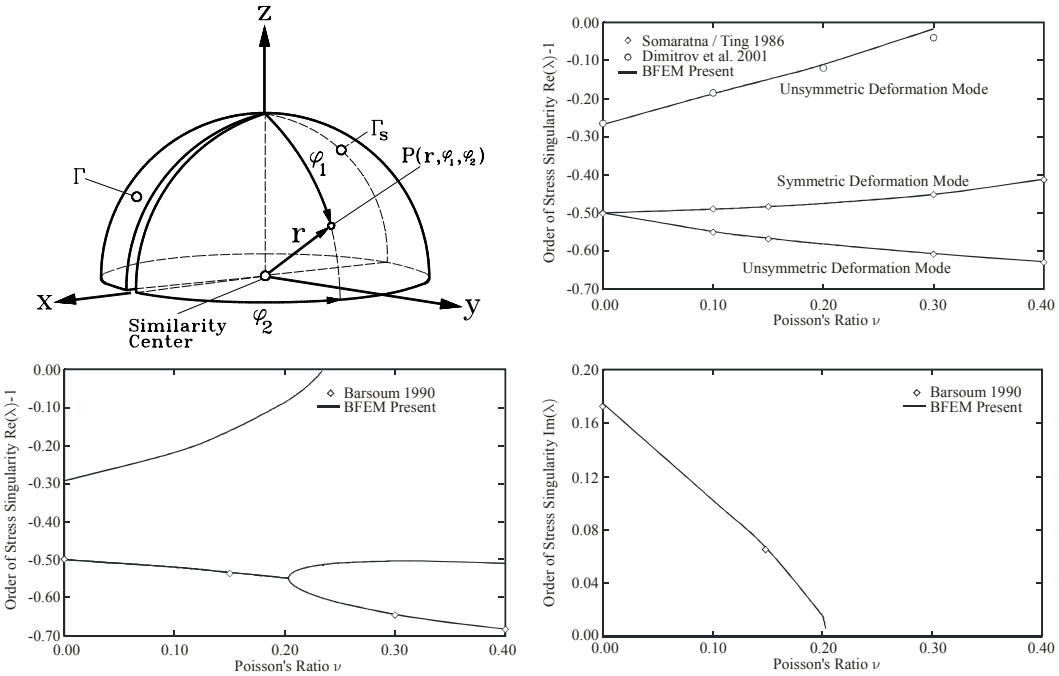

Figure 2: 3D stress singularities at the vertex of a surface breaking crack, upper portion: crack in an isotropic halfspace, lower portion: interface crack between an isotropic halfspace and a rigid substrate.

The situation of an interface crack between an isotropic halfspace and a rigid substrate is simulated by setting $u_r = u_1 = u_2 = 0$ on Γ_s and again only discretizing the surface of the region $r = 1$, $0 \leq \varphi_1 \leq \pi/2$, $0 \leq \varphi_2 \leq \pi$ which is assumed to contain the linear elastic material. The BFEM results are

displayed in fig. 2, lower portion, along with the FEM results as reported by Barsoum [3] with which a good agreement is found. In the range of approximately $0 < \nu < 0.20$ a dominating complex eigenvalue arises which for $\nu > 0.2$ splits into two separate values. At the bifurcation point a logarithmic stress singularity occurs. A further relevant real eigenvalue of lower power arises in the range of about $0 < \nu < 0.24$. Again, the dominating eigenvalue exceeds the typical two-dimensional $r^{-0.5}$-singularity.

2.2 Stress singularities in the vicinity of a free laminate corner

Consider a laminated plate with layers consisting of a typical fibre reinforced plastic (see [8] for details). There is a special interest in information about the occurring stress singularities in the vicinity of free laminate corners (so-called free-corner effect [6-8]) in the interfaces between two dissimilar laminate layers. Let us consider arbitrary corner opening angles $0 \le \gamma \le 2\pi$ (fig. 3, left portion). In the upper layer (layer 1) of the considered bimaterial interface, the fibers are orientated parallel to the global y-axis. The fibers of the lower layer (layer 2) are assumed to run parallel to the global x-axis. We thus consider a so-called cross-ply [90°/0°]-interface. The laminate corner region is situated in the interval r, $0 \le \varphi_1 \le \pi$, $0 \le \varphi_2 \le \gamma$, the planes r, $0 \le \varphi_1 \le \pi$, $\varphi_2 = 0$ and r, $0 \le \varphi_1 \le \pi$, $\varphi_2 = \gamma$ represent the traction free laminate edges. Laminate layer 1 is found in the interval r, $0 \le \varphi_1 \le \pi/2$, $0 \le \varphi_2 \le \gamma$ whereas layer 2 occupies the region r, $\pi/2 \le \varphi_1 \le \pi$, $0 \le \varphi_2 \le \gamma$. The interface between the two dissimilar laminate layers coincides with the xy-plane at $z = 0$. The surface Γ at $r = 1$ has again been discretized with 8-noded quadrangular surface elements wherein the corner tip presently coincides with the similarity center of the BFEM mesh. A mesh refinement was used around the points $r = 1$, $\varphi_1 = \pi/2$, $\varphi_2 = 0$ and $r = 1$, $\varphi_1 = \pi/2$, $\varphi_2 = \gamma$ where the two free-edge interfaces intersect with the BFEM mesh. For corner angles $\gamma > \pi$, a further mesh refinement was applied in the vicinity of the points $x = y = 0$, $z = 1$ and $x = y = 0$, $z = -1$. Reference results for the order of the three-dimensional stress singularities at the corner tip $x = y = z = 0$ are found in e.g. Dimitrov et al. [8] and excellently agree with the present BFEM computations. For corner angles in the interval $0 \le \gamma \le \pi$ only one real relevant eigenvalue arises. This stress singularity is of low order $\lambda - 1$ which is also a well-known experience considering free-edge effects in composite laminates [6]. For corner angles $\gamma > \pi$, two additional stronger eigenvalues occur which also lead to singular stresses in the vicinity of the free laminate corner, at about $\gamma = 13\pi/9$ a fourth relevant eigenvalue occurs. A maximum eigenvalue is found at approximately $\gamma = 11/6\pi$ which is even slightly above the well-known two-dimensional $r^{-0.5}$-singularity.

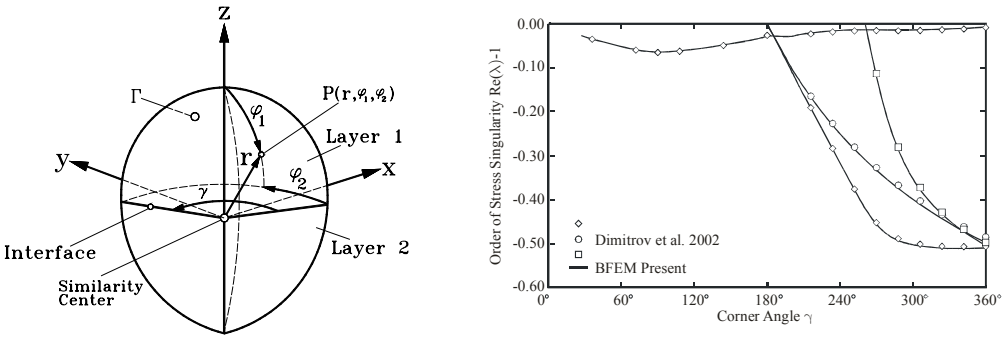

Figure 3: 3D stress singularities at a [90°/0°]-interface at the tip of a free laminate corner with arbitrary opening angle γ.

3 SUMMARY AND CONCLUSIONS

The boundary finite element method (BFEM) has been employed for the semi-analytical computation of the orders of stress singularities for some classes of three-dimensional elasticity problems. In all presented cases the BFEM results agree very well with reference results and thus render the BFEM a powerful tool for the investigation of three-dimensional singular stress concentration phenomena in linear elastic solids. The BFEM requires significantly lower numerical effort in comparison to standard numerical methods like e.g. the finite element method and is thus especially useful for exhaustive parameter studies or optimization procedures.

REFERENCES

[1] J. P. Wolf, C. Song, *Finite-Element Modelling of Unbounded Structures,* John Wiley & Sons Ltd., Chichester et al., England (1996).

[2] N. Somaratna, T. C. T. Ting, *Three-Dimensional Stress Singularities in Anisotropic Materials and Composites*, International Journal of Engineering Science, 24, (1986), 1115-1134.

[3] R.S. Barsoum, *Asymptotic Fields at Interfaces Using the Finite Element Iterative Method*, Computers & Structures, 35, (1990), 285-292.

[4] A. Dimitrov, H. Andrae, E. Schnack, *Efficient Computation of Order and Mode of Corner Singularities in 3D-Elasticity*, International Journal for Numerical Methods in Engineering, 51, (2001), 1-24.

[5] Z. P. Bazant, L. M. Keer, *Singularities of Elastic Stresses and of Harmonic Functions at Conical Notches or Inclusions*, International Journal of Solids and Structures, 10, (1974), 957-964.

[6] C. Mittelstedt, W. Becker, *Interlaminar Stress Concentrations in Layered Structures - Part I: A Selective Literature Survey on the Free-Edge Effect since 1967, Part II: Closed-Form Analysis of Stresses at Laminated Rectangular Wedges with Arbitrary Non-Orthotropic Layup*, Journal of Composite Materials, (2004), in press.

[7] C. Mittelstedt, W. Becker, *A Variational Finite Layer Technique for the Investigation of Thermally Induced Stress Concentrations in Composite Structures,* Journal of Thermal Stresses, (2004), in press.

[8] A. Dimitrov, H. Andrae, E. Schnack, *Singularities near Three-Dimensional Corners in Composite Laminates*, International Journal of Fracture, 115, (2002), 361-375.